

Fasudil Attenuates LPS-Induced Acute Lung Injury by Preventing Endothelial Dysfunction

Jingjing Wang [†], Jian Xu [†], Xinyun Zhao, Weiping Xie, Hong Wang ^{*} and Hui Kong ^{*}

Department of Respiratory & Critical Care Medicine, the First Affiliated Hospital of Nanjing Medical University, Nanjing, Jiangsu 210029, China.

seesea19890102@163.com (J.W.); sparforward@sina.com (J.X.);

zhaoxinyunnj@126.com (X.Z.); wpxie@njmu.edu.cn (W.X.);

hongwang@njmu.edu.cn (H.W.); konghui@njmu.edu.cn (H.K.)

[†] These authors contributed equally to this work

^{*} Correspondence:

Email: hongwang@njmu.edu.cn & konghui@njmu.edu.cn

Tel: +86-25-68136426; Fax: +86-25-68136269

Abstract: Fasudil, a potent Rho kinase (ROCK) inhibitor, can ameliorate LPS-induced acute lung injury (ALI) in mice, but the mechanism remains obscure. In this study, a mice model of ALI was established by intra-tracheal instillation of LPS. Histological changes, cytokine levels, lung permeability, and endothelial apoptosis were determined to evaluate the effects of fasudil on lung injury. The cellular and molecular biological mechanisms were explored by culturing human pulmonary microvascular endothelial cells (PMECs). The results showed that fasudil reduced LPS-induced lung inflammation, pulmonary hyperpermeability, and endothelial apoptosis in mice. In cultured human PMECs, fasudil inhibited LPS-induced caspase-3 cleavage and cell apoptosis. It also decreased LPS-induced hyperpermeability of human PMECs monolayer by reversing the down-regulation of intercellular junctions. Moreover, fasudil inhibited LPS-induced overexpression of chemokines and intercellular adhesion molecule (ICAM)-1 in human PMECs, which in turn suppressed neutrophil chemotaxis and neutrophil-endothelial adhesion. Further molecular researches showed fasudil inhibited LPS-induced activation of ROCK, NF- κ B, and p38 in human PMECs. Our findings demonstrated that fasudil alleviated LPS-induced ALI by protecting endothelial function via inhibiting endothelial apoptosis, maintaining endothelial barrier integrity, and reducing endothelial inflammation. These effects of fasudil could be attributed to the inhibition of ROCK and its downstream NF- κ B and p38 signaling pathways.

Key words: acute lung injury; fasudil, Rho kinase; endothelial function; inflammation

1. Introduction

Acute lung injury (ALI) or acute respiratory distress syndrome (ARDS), induced by various infectious and noninfectious insults with a complex pathogenesis, is a fatal clinical syndrome with high morbidity and mortality in critically ill patients [1]. It is generally accepted that ALI involves inflammation injury to the alveolar-capillary barrier, resulting in increased lung permeability, accumulation of protein-rich pulmonary edema fluid, neutrophil entrapment and activation in the airspaces [1-3]. These pathological abnormalities lead to deficient gas exchange, arterial hypoxemia, and respiratory failure that define clinical ALI.

In the inner walls of pulmonary capillary, neighboring endothelial cells are tightly connected to each other by intercellular junctions, constituting a continuous endothelial cell monolayer, one semi-permeable barrier between blood and interstitium [4]. Under normal physiologic conditions, this endothelial monolayer maintains the homeostasis of lung interstitial fluid through dynamically controlling the transcellular extravasation of cells, proteins, and fluids [5]. However, as the primary target of inflammation, endothelia is vulnerable to damaging insults, such as pneumonia and sepsis that invade via the alveolar or vascular lumen. Bacterial toxins rapidly compromise endothelial cell function, leading to disruption of endothelial barrier integrity and subsequent pulmonary hyperpermeability [6,7]. Based on these facts, it is reasonable that protecting endothelial function could be a novel therapeutic strategy [2]. However, no specific pharmacologic therapy to date is available to improve endothelial function in the treatment of ALI.

ROCK, a serine/threonine kinase, is a downstream effector of Rho family small GTPases. Mounting evidence has shown that ROCKs act as determinant molecular switches controlling several critical cellular functions, such as proliferation and apoptosis, cytoskeletal rearrangement, cell adhesion and migration, inflammation, and reactive oxygen species formation [8-10]. Fasudil, a potent and selective ROCK inhibitor, showed clinical effectiveness and safety in the treatments of cardiovascular and cerebrovascular diseases, such as aneurysmal subarachnoid hemorrhage and myocardial ischemia [11,12]. Some experimental and clinical studies on respiratory diseases have shown that fasudil would be a prospective drug for the treatment of pulmonary fibrosis [13] and pulmonary arterial hypertension [14-16]. Moreover, it was reported that fasudil prevented sepsis-induced ALI by inhibiting system inflammation *in vivo* [17] and lipopolysaccharide (LPS)-induced apoptosis of rat PMECs *in vitro* [18]. However, the effects of fasudil on LPS-induced ALI and the underlying mechanisms remain poorly understood.

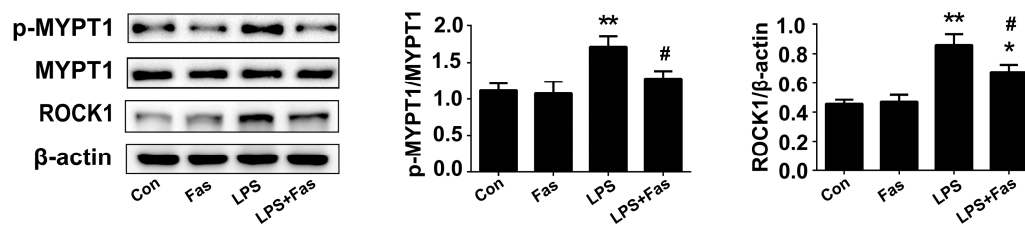
In the present study, a murine model of ALI induced by intra-tracheal instillation of LPS and cultured human PMECs were used to investigate the protective effects of fasudil and its potential cellular and molecular mechanisms underlying.

2. Results

2.1. Fasudil inhibited LPS-induced Rho/ROCK activation in lung

Lung tissues of mice were harvested to investigate the effects of LPS and fasudil on ROCK activation. The expressions of ROCK isoforms (ROCK1 and ROCK2) and

activation of downstream myosin phosphatase target (MYPT)-1 were examined by western blotting. We showed that LPS challenge led to a significant up-regulation of phosphorylated MYPT-1 (p-MYPT1) and ROCK1 in lungs (Figure 1). However, these effects of LPS were significantly inhibited by pretreatment with 10 mg/kg fasudil.



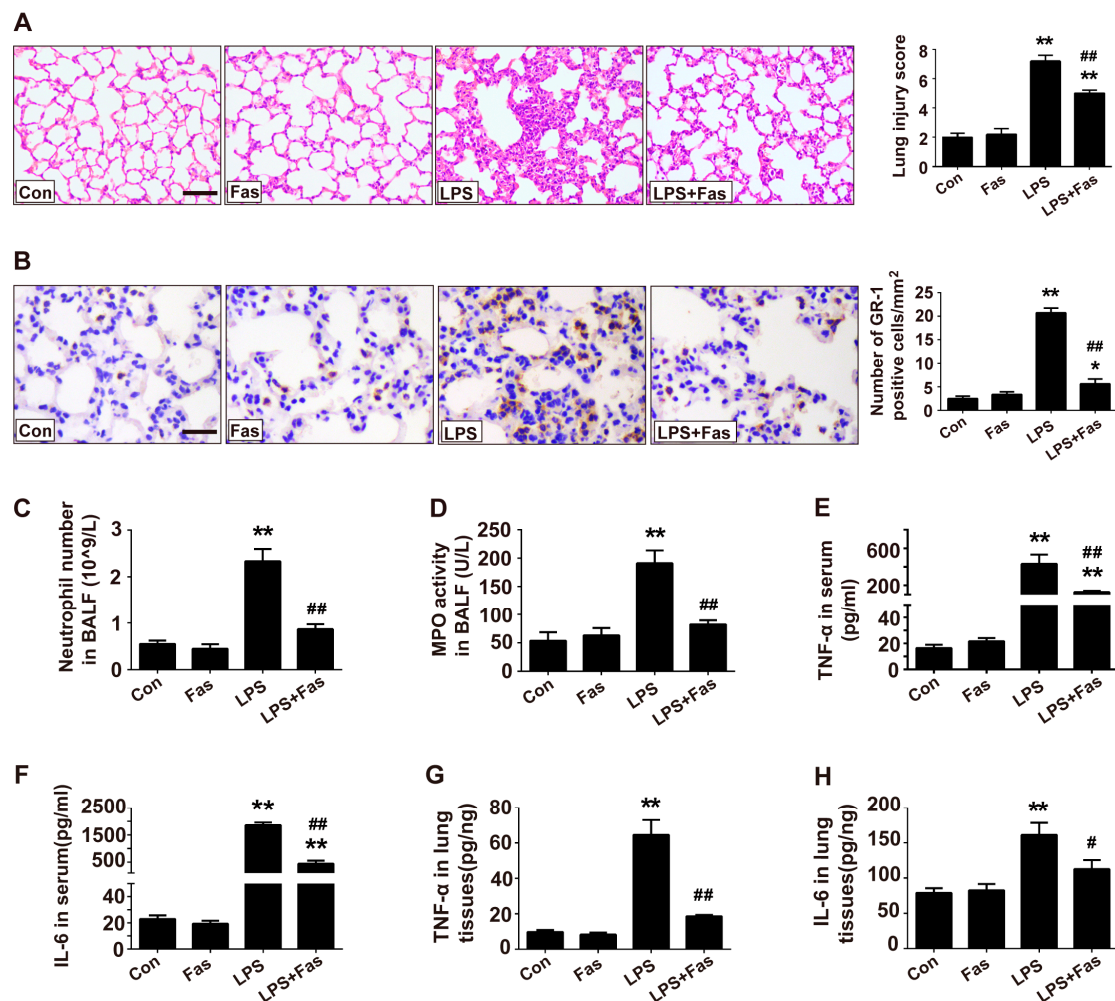
2.2. Fasudil ameliorated LPS-induced ALI and inflammation

To characterize the role of fasudil in LPS-mediated lung injury, lung histological changes were analyzed by an established scoring system [19]. Briefly, lung injury scores are positively correlated with alveolar septal congestion, alveolar hemorrhage, intra-alveolar fibrin deposition, and intra-alveolar infiltrates, which means a higher score represents more serious lung injury. As indicated in Figure 2A, compared with control mice, intra-tracheal instillation of LPS resulted in significant lung injury, which was alleviated by fasudil pretreatment.

Immunohistochemistry staining of Gr-1, a marker of mature neutrophil, showed that LPS-induced neutrophil infiltration in lung interstitium and alveolar space was markedly attenuated by fasudil pretreatment (Figure 2B). This result was further validated by measuring the neutrophil numbers and MPO activities in BALF. As shown in Figure 2C and D, fasudil reversed LPS-induced increments of neutrophil

numbers and MPO activities in BALF.

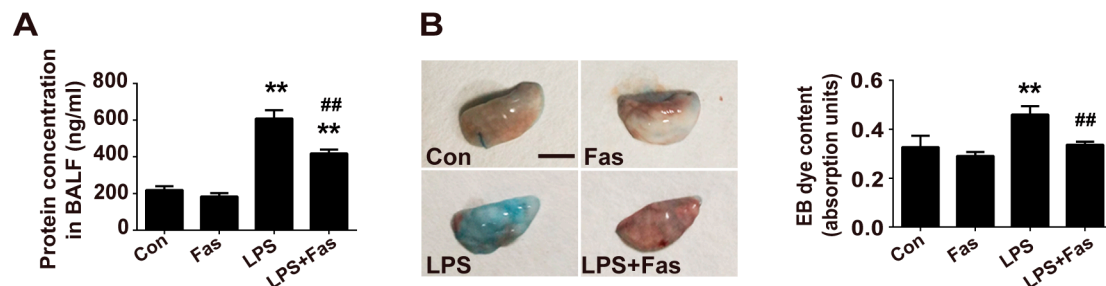
TNF- α and IL-6 were measured to investigate the inflammatory response in lungs of mice. As indicated in Fig. 2E~H, fasudil pretreatment significantly decreased LPS-induced high levels of TNF- α and IL-6 either in serum or in lung homogenates.



2.3. Fasudil reduced lung hyperpermeability induced by LPS

Lung hyperpermeability is a hallmark of ALI. Therefore, the protein level in BALF was measured to analyze the severity of lung permeability. As shown in Figure 3A, pretreatment of fasudil significantly inhibited the increase of protein level in BALF after LPS administration.

We further evaluated lung permeability by injecting EB intraperitoneally. As shown in Figure 3C, LPS markedly increased lung vascular leakage as indicated by the elevated level of EB in lungs, while it was reversed by pretreatment with fasudil.



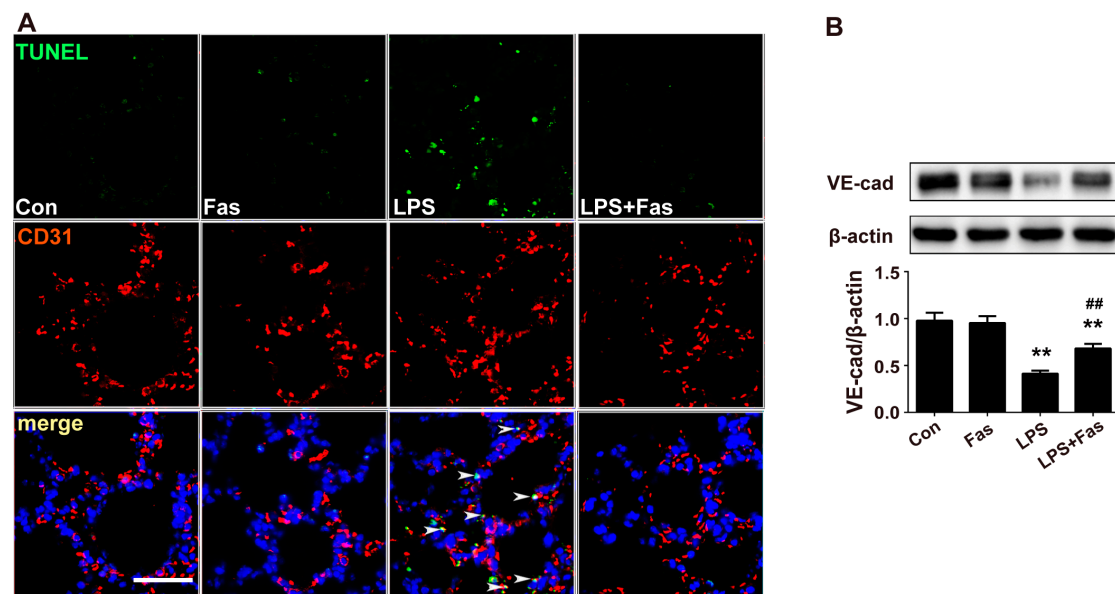
2.4. Fasudil protected lung endothelial cells against LPS-induced dysfunction *in vivo*

PMECs dysfunction brings about the collapse of endothelial barrier, and subsequent lung hyperpermeability [20]. Therefore, we first examined endothelial cell apoptosis using TUNEL and CD31 immunofluorescence staining. As shown in Figure 4A, a number of TUNEL positive and CD31 positive (TUNEL⁺/CD31⁺) cells (apoptotic PMECs) were observed in lungs of LPS-treated mice. However, barely TUNEL⁺/CD31⁺ cell was found in both control group and LPS + fasudil group.

Vascular endothelial (VE)-cadherin is an endothelial-specific adhesion molecule essential to maintain vascular barrier function. As shown in Figure 4B, western blot analysis demonstrated a significant down-regulation of VE-cadherin in the lungs of LPS-challenged mice. Although fasudil itself had no effect on the expression of VE-cadherin, it partially reversed LPS-induced down-regulation of VE-cadherin in the lungs of mice.

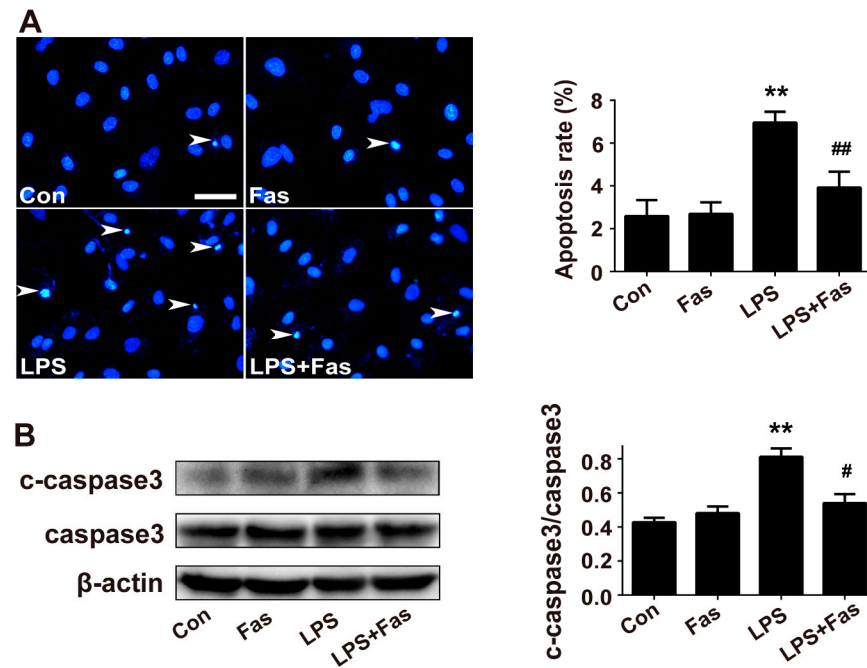
Together, these results strongly suggested that fasudil could attenuate LPS-induced ALI by protecting endothelial cells. Thus, *in vitro* studies were carried

out to further evaluate the effect of fasudil on LPS-challenged human PMECs.



2.5. Fasudil reversed LPS-induced cultured human PMECs apoptosis

As indicated in Figure 5A, apoptotic nuclei with chromatin condensation and nuclear fragmentation were more easily to be dyed, and showed brilliant blue fluorescence, while non-apoptotic nuclei showed light blue fluorescence. Statistical analysis demonstrated that fasudil itself did not trigger PMECs apoptosis, but it reversed LPS-induced human PMECs apoptosis. To further confirm this finding, the activation of caspase-3, one critical executioner of apoptosis, was examined. Similarly, fasudil pretreatment potently inhibited LPS-induced caspase-3 cleavage/activation in human PMECs (Figure 5B).

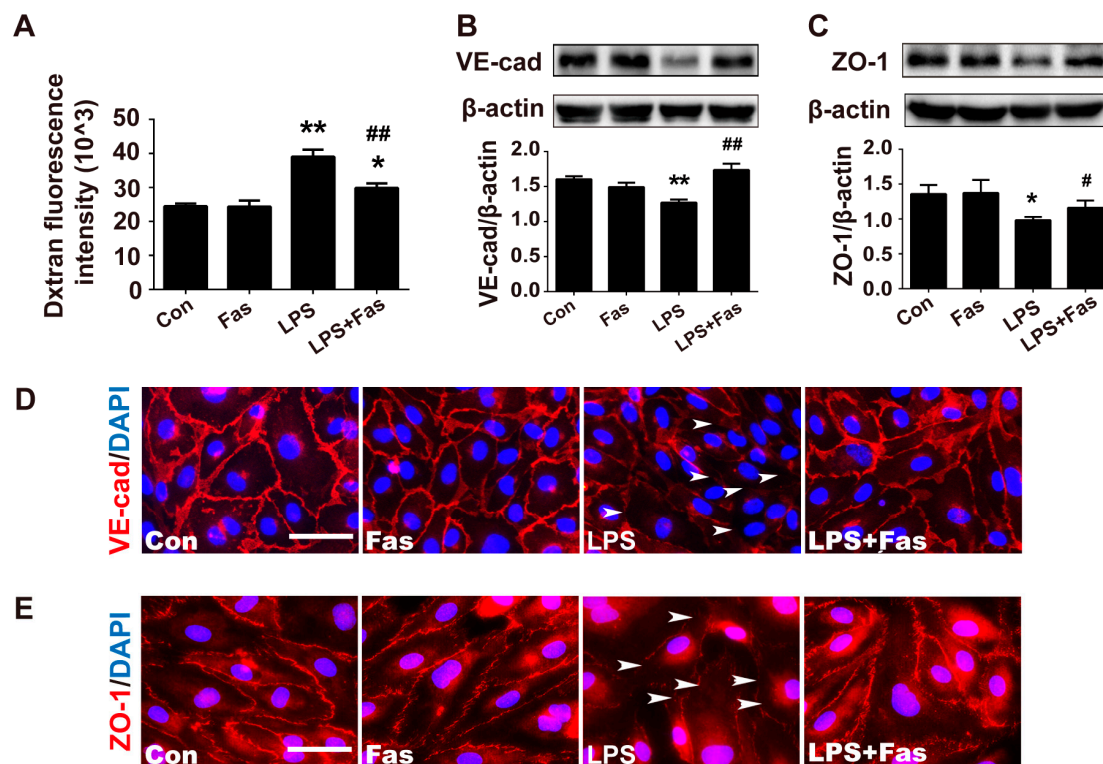


2.6. Fasudil recovered LPS-induced human PMECs hyperpermeability

In a transwell system, FITC-dextran permeating through the monolayer of cultured human PMECs was measured to evaluate the endothelial barrier permeability *in vitro*. The results showed that LPS challenge for 24 h significantly enhanced permeability of human PMECs monolayer for FITC-dextran than the control group (Figure 6A). Fasudil alone had no influence on basal permeability, while it decreased LPS-induced hyperpermeability of human PMECs monolayer.

Adherens junctions (AJs) and tight junctions (TJs) expressed in endothelial cells are vital to control endothelial permeability. Thus, the expressions and distribution of key molecules for AJs (VE-cadherin) and TJs (zonula occludens[ZO-1]-1) in human PMECs were examined. Our data showed that LPS challenge for 24 h significantly down-regulated expressions of VE-cadherin and ZO-1 (Figure 6B and C) in human PMECs, while these down-regulations were reversed by fasudil. Accordingly,

immunofluorescence staining further confirmed that pretreated with fasudil prevented LPS-induced loss of VE-cadherin and ZO-1 at cell-cell junctions (Figure 6D and E).



2.7. Fasudil suppressed neutrophil chemotaxis and adhesion mediated by LPS-stimulated human PMECs

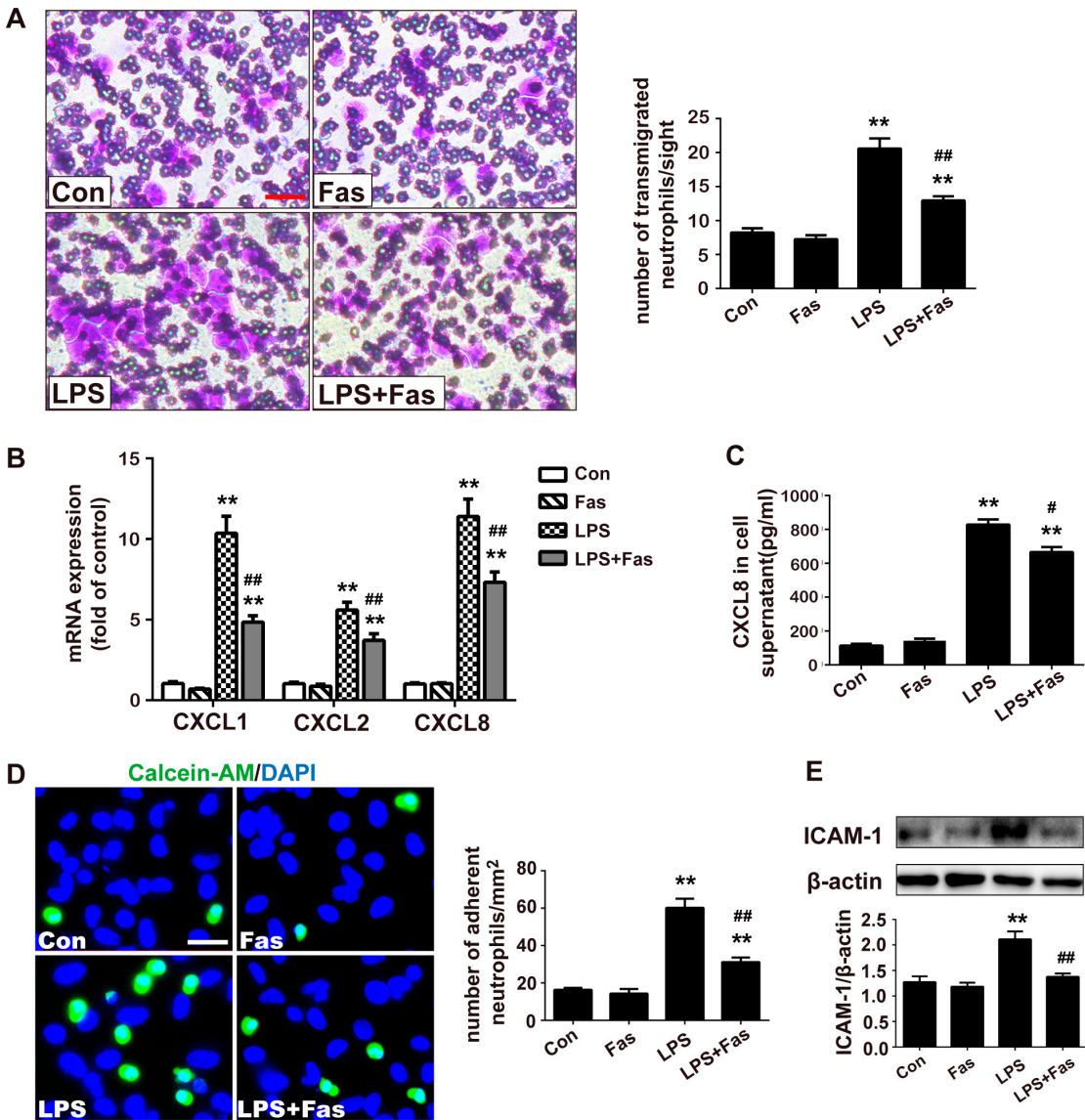
Neutrophil chemotaxis assay showed that a large number of neutrophils transmigrated onto the lower side of transwell filter when human PMECs in the lower chamber were stimulated by LPS (Figure 7A). However, the trans-filter migration of neutrophils was significantly inhibited when LPS-stimulated human PMECs were pretreated with fasudil in the lower chamber.

Since activated human PMECs could synthesize and release chemokines to facilitate neutrophil migration, the expressions of CXCL-1, CXCL-2 and CXCL-8 by human PMECs were detected. qRT-PCR analysis showed LPS induced significant

transcription of all these three chemokines in human PMECs (Figure 7B), which was attenuated by fasudil. Consistently, ELISA confirmed that fasudil significantly inhibited LPS-induced CXCL8 protein releasing from human PMECs (Figure 7C).

Neutrophil-endothelial adhesion is a critical step in the development of inflammatory diseases [21,22]. Thus, neutrophils and human PMECs were cocultured to investigate the effect of fasudil on LPS-induced neutrophil-endothelial adhesion. As indicated in Figure 7D, LPS significantly promoted neutrophil-endothelial adhesion, which was attenuated by fasudil pretreatment.

Neutrophil-endothelial adhesion is mediated by several adhesion molecules, especially intercellular adhesion molecule-1 (ICAM-1). Western blot analysis showed that fasudil completely reversed LPS-induced overexpression of ICAM-1 in human PMECs (Figure 7E).



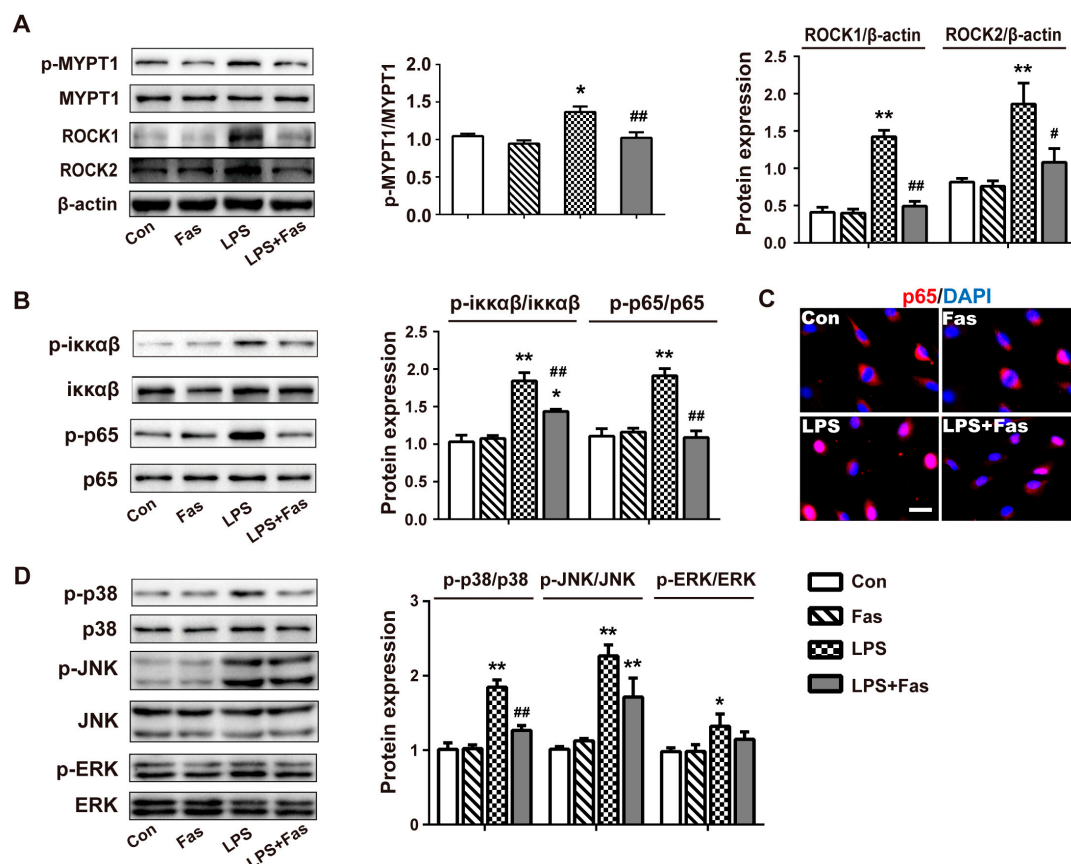
2.8. Fasudil inhibited Rho/ROCK, NF- κ B, and p38 MAPK activation in LPS-challenged HPMECs

To reveal the molecular mechanism for the protective effects of fasudil in endothelial dysfunction, ROCK, NF- κ B, and MAPK signals involving the regulation of cell permeability, apoptosis, and inflammation were examined. Our results showed LPS induced rapid MYPT-1 phosphorylation at 30 min, and led to overexpression of ROCK1/ROCK2 at 24 h (Figure 8A). However, LPS-stimulated ROCK activation

was completely suppressed by fasudil pretreatment.

As to NF- κ B signaling, the phosphorylation of p65 and $\text{ik}\kappa\alpha\beta$ were significantly enhanced in LPS-challenged human PMECs (Figure 8B), which were reversed or suppressed by the pretreatment of fasudil. Moreover, immunofluorescence staining showed that fasudil pretreatment significantly inhibited NF- κ B p65 nuclear translocation induced by LPS (Figure 8C).

For MAPK signaling, as shown in Fig. 8D, LPS triggered significant phosphorylation of p38 and JNK, and moderate phosphorylation of ERK in human PMECs. Interestingly, fasudil completely reversed LPS-elicited p38 phosphorylation, but neither JNK nor ERK phosphorylation.



3. Discussion

As the hallmark of ALI, lung vascular hyperpermeability is caused by endothelial dysfunction, which in turn results in pulmonary oedema and inappropriate accumulation of activated leukocytes in the interstitium and alveolar space. Exposure of the lower respiratory tract to LPS by intra-tracheal instillation is a well-documented animal model of ALI, which mimics pathological aspects of clinical development of ALI induced by pulmonary inflammation without causing systemic inflammation and multi-organ failure [23,24]. In this study, our results suggest that fasudil, a potent ROCK inhibitor, inhibits LPS-induced ALI by preventing LPS-induced endothelial dysfunction via the following mechanisms: 1) protecting endothelial cells from LPS-induced apoptosis; 2) restoring endothelial barrier integrity and decreasing endothelial permeability; and 3) reducing endothelial inflammation.

The microvascular endothelium is the first barrier to be encountered by fluid or inflammatory cells tracking from vasculature to alveoli in the development of ALI. PMECs are elementary components of lung microvascular that control the function of capillary membrane barrier under both physiological and pathological conditions. Death of PMECs causing loss of lung endothelium integrity has been proposed as an important mechanism for septic lung microvascular dysfunction [1]. Mounting evidence demonstrated that PMECs were highly vulnerable to apoptosis induced by detrimental stimuli such as LPS, TNF- α , and oxidative stress either *in vitro* or *in vivo*. Recently, it was confirmed that apoptosis-mediated death of PMECs contributed to pulmonary microvascular barrier dysfunction in murine models of sepsis-induced ALI

[25]. In the present study, we showed that fasudil protected pulmonary endothelial cells against LPS-induced apoptosis both *in vivo* and *in vitro*. Moreover, in cultured human PMECs, fasudil sufficiently inhibited LPS-induced activation of apoptosis executor caspase-3, accompanied by ROCK activation. Inhibition of the ROCK pathway by fasudil has been reported to prevent apoptosis through direct or indirect inhibition of caspase-3 [26,27]. Previous studies have suggested that ROCK activation evoked caspase-3 cleavage via up-regulating the expression of Bax and Bclxl [28] and depending on myosin-mediated contraction [29] in different cell types. Although the mechanism by which inhibition of ROCK affects caspase-3 activation remains unclear, our results indicate that ROCK activation may act as an upstream event required for caspase-3 cleavage in LPS-induced human PMECs apoptosis.

Besides endothelial apoptosis mediated loss of endothelial barrier integrity, disruption of endothelial cell-cell adhesion also leads to microvascular hyperpermeability during ALI. It is now well recognized that loss of endothelial cell-cell adhesion is sufficient to induce the formation of inter-endothelial cell gap which provide paracellular pathway for free passage of macromolecules through the endothelial barrier [30,31]. Several types of cellular junctions, such as tight junctions (TJs), adherens junctions (AJs) and gap junctions, participate in inter-endothelial adhesion. Among these junctions, TJs and AJs are implicated to be involved in the regulation of paracellular permeability. In our *in vitro* study, fasudil significantly decreased LPS-induced FITC-dextran leakage through the monolayer of cultured human PMECs in a transwell system, indicating that fasudil could alleviate

endothelial paracellular hyperpermeability under endotoxin stress. Furthermore, western blot and immunofluorescence analysis showed that fasudil reversed the down-regulation of ZO-1 and VE-cadherin induced by LPS in human PMECs. Thus, these results suggest that fasudil could maintain the barrier function of endothelial cells by restoring inter-endothelial TJs and AJs. Recently, it was reported that LPS induced the redistribution and loss of VE-cadherin in human lung microvascular endothelial cells via Rho/ROCK signaling pathway [32]. Moreover, in the past decade, accumulating evidence has indicated that Rho/ROCK activation by different insults resulted in disarrangement and down-regulation of both VE-cadherin and ZO-1 in endothelial cells of brains [33], intestines [34] or umbilical veins [35], which may be attributed to the formation of actin stress fiber that is responsible for actomyosin cell contractility [35]. Thereby, maintaining inter-endothelial junctions by inhibiting ROCK activation could occupy a central position in decreasing the endothelial paracellular permeability in ALI.

Overwhelming inflammation characterized by massive inflammatory cells infiltration and mediators release is another feature of ALI. Endothelia is also a principle component involved in systemic or multiple organic inflammation. Under normal conditions, quiescent endothelial cells regulate inflammatory processes in blood vessels to very low levels, owing to the expression of anti-inflammatory molecules [36]. However, in response to noxious stimuli (such as bacterial endotoxins, persistent hypoxia, and ischemia), endothelial cells transform into pro-inflammatory phenotypes subsequently to release cytokines/chemokines and recruit leucocytes to

the site of tissue injury or infection [37]. In our *in vivo* study, fasudil significantly decreased the levels of cytokines (TNF- α and IL-6) and reduced neutrophil exudation in lungs of LPS-treated mice, indicating that fasudil could effectively inhibit LPS-challenged inflammatory cells infiltration and subsequent lung injury. During the development of ALI, endothelial cells can be induced to express chemokines and adhesion molecules mediating neutrophils attachment on and migration through endothelium into lung parenchyma. Chemokines are the largest family of cytokines including four canonical subclasses, being CC, CXC, and CX₃C, XC [38]. Among them, CXC chemokines exert most potent neutrophil chemotactic and activating properties both *in vitro* and *in vivo* [39]. Regarding chemokine ligands, CXCL1, CXCL2, and CXCL8 are recognized as important CXC chemokines in both experimental and clinical ALI. In our *in vitro* study, fasudil pretreatment significantly inhibited the overexpressions of CXCL1, CXCL2, and CXCL8 in LPS-challenged human PMECs, and attenuated neutrophil chemotaxis in a non-contact transwell coculture system. These results implicated that inhibiting ROCK by fasudil could prevent endothelial-mediated inflammation via suppressing inflammatory cell chemotaxis. In addition, in a contact coculture system, fasudil inhibited neutrophil adhesion to LPS-stimulated human PMECs. Since ICAM-1 promotes neutrophil-endothelial adhesion, this effect may be attributed to the downregulation of ICAM-1 in LPS-challenged human PMECs by fasudil. Consistently, it has been reported that ROCK regulated ICAM-1 expression by virtue of controlling the downstream NF- κ B signaling in endothelial-mediated inflammation [40,41]. Together,

attenuating endothelial cell inflammation could be one of the mechanisms for fasudil to prevent LPS-induced ALI.

It is well established that NF- κ B pathway is engaged in endothelial barrier dysfunction in LPS-induced lung injury. Pharmacological inhibition of NF- κ B activation suppressed LPS-induced apoptosis, cytokine release, and adhesion molecule expression in endothelial cells *in vitro*, and alleviated LPS-induced ALI *in vivo* [42]. Thus, NF- κ B signaling was examined to elucidate the potential molecular mechanism underlying the protective effects of fasudil in LPS-induced endothelial dysfunction. Our results showed that LPS resulted in NF- κ B activation in human PMECs, as indicated by pronounced phosphorylation of $\text{I}\kappa\text{B}\alpha$ and NF- κ B p65, as well as nuclear translocation of p65. However, these effects were suppressed by the selective ROCK inhibitor fasudil. Although whether the effects of fasudil are mediated by acting on NF- κ B directly is unknown, it is well documented that ROCK is involved in NF- κ B activation in endothelial cell during inflammation [41,43]. Two isoforms of ROCK have been described and are widely referred to as ROCK1 and ROCK2. By using small interfering RNA-facilitated knockdown of each isoform, Shimada *et al.* identified ROCK2 activation as being the early event driving NF- κ B activation and the subsequent transcriptional upregulation of chemokines and ICAM-1 in human endothelial cells treated with proinflammatory lysophosphatidic acid [43]. By using pharmacological approaches, Anwar *et al.* demonstrated that ROCK1 mediated thrombin-induced NF- κ B activation in endothelial cells by enhancing phosphorylation of the transactivation domain of RelA/p65 [41]. In our

study, fasudil potently inhibited LPS-induced upregulation of both ROCK1 and ROCK2, and downstream phosphorylation of MYPT-1 in human PMECs. Thereby, as discussed above, it is reasonable that fasudil could attenuate LPS-induced endothelial dysfunction through inactivation of ROCK-dependent NF- κ B pathway.

In addition to NF- κ B, MAPKs signaling pathways, including p38, ERK1/2, and JNK, also participate in LPS-induced endothelial injury [44]. It is noteworthy that these three kinases may have different functions in LPS-induced endothelial barrier dysfunction. Exactly, p38 activation critically contributes to endothelial apoptosis, cytokines and chemokines production, and ICAM-1 expression, while JNK activation mainly mediates endothelial apoptosis. The activation of ERK1/2 in response to LPS has not been well characterized. Several reports implicate that ERK1/2 regulates endothelial inflammation, apoptosis, and cell proliferation in response to LPS challenge. In the present study, we found that LPS challenge for 30 min induced a significant phosphorylation of both p38 and JNK, but only a moderate phosphorylation of ERK1/2 in human PMECs. This discrepancy may be attributed to their distinctive spatiotemporal activation patterns. In rat PMECs, it was reported that LPS could elicit an early and robust activation of p38 and JNK with the peak value at 30 min after treatment, while the activation of ERK1/2 reached the peak at 60 min [18]. Additionally, we found that pretreated with fasudil significantly inhibited LPS-induced activation of p38 in human PMECs, but had no significant effect on the activation of JNK and ERK1/2. By using fasudil, the relationship between ROCK and MAPKs has been investigated in various cells [18,45,46] suggesting that ROCK may

regulate MAPKs signal transduction in a time- or cell-specific manner. In terms of the current study, our results suggest that p38, but not JNK or ERK1/2 might serve as the early downstream molecules of ROCK signal pathway in human PMEC dysfunction induced by LPS.

4. Materials and Methods

4.1. Animal model of ALI

All experimental protocols were approved by the Institutional Animal Care and Use Committee of Nanjing Medical University and were in accordance with the guidelines of the National Institutes of Health. Male C57BL/6 mice (20~22 g, Changzhou Cavans Lab. Animal Corporation Ltd. China) were orally intubated with a sterile plastic catheter after anesthesia, and then challenged with intra-tracheal instillation of LPS (5mg/kg; Sigma-Aldrich, St. Louis, MO, USA) dissolved in 50 μ l of normal saline or saline alone as the control. Fasudil (10 mg/kg; Sigma-Aldrich) was given 1 h before LPS administration. At the point of 24 h after LPS administration, mice were killed for sample collection (n = 8 for each group).

4.2. Lung histological examination

The left lung tissues were stained with Hematoxylin-and-eosin (H&E). For each section, a minimum of 10 randomly chosen areas were analyzed by microscopy (Laica, Germany) at 200 magnification. The degree of lung injury was assessed by a semi-quantitative scoring system depending on previous investigators [19].

4.3. Measurement of inflammatory cytokines and chemokine

Concentrations of TNF- α and IL-6 in serum and lung tissues were measured with murine cytokine-specific ELISA kits (R&D Systems, Minneapolis, MN) according to manufacturer's instructions. The levels of cytokines (TNF- α , IL-6) in lungs were normalized by corresponding protein concentrations. CXCL8 in supernatant of human PMECs was measured according to the common protocol.

4.4. Measurement of leukocyte influx, protein content and myeloperoxidase activity

Neutrophils in BALF were counted using a haemocytometer immediately. Protein content in BALF was measured with Bicinchoninic Acid (BCA) assay kit (Beyotime, China) according to the instructions. Myeloperoxidase (MPO) activity in BALF was measured with a commercial test kit (Jiancheng Bioengineering Institute Nanjing, China) following the manufacturer's directions.

4.5. Immunohistochemistry and immunofluorescence staining

The deparaffinized sections were coped with antigen retrieval and endogenous peroxidase removal, and human PMECs having been seeded into an 8-well coverslip (Millicell EZ) were fixed in methanol. After 1 h of blocking with 2% BSA, the sections or coverlip were incubated with primary antibodies against Gr-1 (10 μ g/ml, Novus Biologicals, Littleton, CO), CD31 (1:200, Santa Cruz Biotechnology), VE-cadherin (1:200, Abcam), ZO-1 (1:200, Proteintech, Rosemont, IL) or NF- κ B p65

(1:100, Cell Signal Technology, Danvers, MA) followed by incubation with HRP-conjugated goat anti-rat (1:1000, Proteintech) or goat anti-rabbit Alexa Fluor 555-conjugated IgG antibody (1:2000, Thermo fisher scientific), respectively. For each section, the number of positive staining cells was counted in 10 different fields randomly under a light microscope or fluorescence microscopy (Laica, Germany).

4.6. Terminal deoxynucleotidyl transferase-mediated dUTP Nick End Labeling (TUNEL) assay

After incubation with goat anti-rabbit Alexa Fluor 555-conjugated IgG antibody for labeling microvascular endothelial cells, these sections were stained with TUNEL assay kit (*In Situ* Cell Death Detection Kit, POD, Roche Company, Germany) according to the manufacturer's protocol. Then nuclei of all sections were stained with 0.2 mg/ml DAPI (4, 6-diamido-2-phenylindole hydrochloride) for 15 min. The images were taken under a confocal microscopy (Zeiss, Oberkochen, Germany) and manifested by Photoshop software.

4.7. Permeability of Evans blue dye

Lung permeability was examined as described by Long *et al.* [47]. In brief, mice were intraperitoneally injected with 20 mg/kg 1% Evans blue (EB) dye (containing 4% bovine serum albumin) 4 h prior to sacrifice. After animals were killed, the flushed lungs were photographed and entire lungs were weighted and frozen in liquid nitrogen. Then they were homogenized in formamide (1ml/100mg lung) and

incubated for 24 h at 37°C. Homogenates were clarified by centrifugation at 12,000 g for 20 min and the absorbance of 200 µl clarified supernatant for each sample was measured at 620nm in a 96-well plate.

4.8. Cell Culture

Human PMECs were purchased from Sciencell Research Laboratories (Carlsbad, CA, USA). Cells were cultured at 37°C with 5% CO₂ in EGM (Sciencell, USA) containing 1% penicillin, streptomycin, endothelial cell growth factors and 5% fetal bovine serum (Sciencell, USA). Cells between passage 4 to 6 were used for all experiments. After starvation for 6 h, cells were exposed to LPS (1 µg/ml) with or without fasudil (1 µg/ml) and further cultured for indicated time intervals.

4.9. Assessment of human PMEC permeability

Human PMECs seeded onto 12-well inserts (0.4 µm pore size) were dividedly treated with or without fasudil (1 µg/ml) when they grew completely confluent. After that, cells were incubated with LPS for 24 h. Then 250 µg FITC-dextran (molecule weight, 4000kDa; Sigma- Aldrich) was added into the upper chamber. Two hours later, leakage of FITC-labeled dextran was quantified by measuring fluorescence intensity of 200 µl of each sample from the lower chamber with a fluorescence microplate reader (Biotek, USA).

4.10. Neutrophil chemotaxis assay

Human neutrophils were isolated from peripheral blood of healthy volunteers with Ficoll-Paque Plus (GE Healthcare, Pittsburgh, USA) as described previously [48]. The volunteers in this study were recruited from the First Affiliated Hospital of Nanjing Medical University. Written informed consents were obtained from all participants and their privacy rights were observed. This experiment was approved by the Medical Ethical Review Committees at the First Affiliated Hospital of Nanjing Medical University. Neutrophil chemotaxis was performed in a 12-well Corning transwell system (3- μ m pore size, 6.5-mm diameter). When the human PMECs in the lower chamber reached 70~80% confluency, they were exposed to LPS for 24 h with or without fasudil (1 μ g/ml) pretreatment. Then neutrophils (10^5 cells) isolated from healthy volunteers were added into the upper chambers. The transwell chamber system was incubated at 37°C for 45 min. Upon the incubation period, the top side of the upper chamber was wiped carefully. The cells which migrated through the pores onto the lower side of the membrane were fixed and stained with Diff-Quick. Then, they were counted under a phase contrast microscope (Nikon, Tokyo, Japan) and recorded at more than ten random fields in each group.

4.11. Reverse transcription and quantitative Real-Time PCR (qRT-PCR)

Total human PMECs RNA was extracted with Trizol reagent (Gibco BRL, Grand Island, NY, USA). Reverse transcription was performed with 500 ng of total RNA with SYBR®Premix Ex Taq™ (TaKaRa, Japan). Quantitative RT-PCR was

performed with Eppendorf Mastercycler EP Realplex Real-time PCR System. Two-step RT-PCR was used to perform relative quantification of mRNA. The RT-PCR primer sequences (Homo) are listed as following. The $2^{-\Delta\Delta Ct}$ method was used to quantify mRNA expression relative to GAPDH.

gene	Forward primer	Reverse primer
CXCL1	TTTCTGAGGAGCCTGCAACA	GCACATACATTCCCCTGCCT
CXCL2	GAAAGCTTGTCTCAACCCCG	ACATTAGGCGCAATCCAGGT
CXCL8	GGCAGCCTTCCTGATTTC	AAACTTCTCCACAACCCTCTG
GAPDH	GGACCTGACCTGCCGTCTAG	GTAGCCCAGGATGCCCTTGA

4.12. Neutrophil-endothelial adhesion assay

Neutrophil-endothelial adhesion assay was evaluated using an established coculture system as previous investigators described [49]. After pretreatment with fasudil for 30 min, human PMECs were exposed to LPS for 12 h. The isolated neutrophils were resuspended (10^6 cells/ml) and stained with 4 ng/ml Calcein-AM (BD Biosciences) for 30 min. Then the labeled neutrophils (2×10^5 cells/ml, 500 μ l per well) were coincubated with pretreated human PMECs for 1 h at 37°C. Non-adherent neutrophils were washed out and the number of adherent neutrophils in ten random areas of each well was counted under a fluorescence microscopy (Laica, Germany)

4.13. Western blotting

Protein expression in lung tissues and human PMECs were examined by western blot with primary antibodies against ROCK1/2, ZO-1 (1:1000, Proteintech, Rosemont,

IL), VE-cadherin (1:1000, Abcam), p-MYPT-1/MYPT-1, NF- κ B p-p65/p65, p- $\text{I}\kappa\text{B}\alpha$ /p- $\text{I}\kappa\text{B}\alpha$, p-p38/p38, p-JNK/JNK, p-ERK/ERK, ICAM-1, cleaved caspase-3/caspase-3 (1:1000, Cell Signaling Technology, Danvers, MA) and β -actin (1:5000, Proteintech) followed by HRP-conjugated goat anti-rabbit or goat anti-mouse antibody (1:10000, Proteintech). Densitometric quantification was performed using Image Lab software.

4.14. Statistical analysis

Values were expressed as mean \pm SEM. Differences among multiple groups were determined by one-way ANOVA analysis followed by LSD. $P < 0.05$ was considered statistically significant. All *in vitro* independent experiments were repeated more than three times.

5. Conclusions

our studies suggest fasudil attenuates LPS-induced ALI through protecting endothelial cells from apoptosis, decreasing endothelial hyperpermeability and suppressing endothelial-mediated inflammation. These effects of fasudil could be attributed to the inhibition of ROCK and its downstream NF- κ B and p38 signaling pathways. Our data also indicates that ROCK may be a promising target for blocking the progression of sepsis- or infection-related ALI. However, it should be mentioned here that this study only explored the prophylactic effects of fasudil in LPS-induced ALI. Whether fasudil has therapeutic effects in an established model of ALI requires further investigation.

Acknowledgments: This study was supported by the National Natural Science Foundation of China (No. 81273571), the Jiangsu Clinical Research Center for Respiratory Diseases Project under grant BL2012012, and a Project Funded by the Priority Academic Program Development of Jiangsu Higher Education Institutions (PAPD) (JX10231802).

Author Contributions: JW, JX and HK designed and performed the research; JW, JX, XZ and HK analysed the data; HK, WX and HW interpreted results of experiments; JW and HK wrote the paper and HK, WX and HW revised the paper.

Conflict of Interests: The authors declare that they have no competing interests.

References

1. Fanelli V, Ranieri VM. Mechanisms and clinical consequences of acute lung injury. *Annals of the American Thoracic Society*. **2015**; 12 Suppl 1: S3-8.
2. Muller-Redetzky HC, Suttorp N, Witzenrath M. Dynamics of pulmonary endothelial barrier function in acute inflammation: mechanisms and therapeutic perspectives. *Cell and tissue research*. **2014**; 355: 657-73.
3. Herold S, Gabrielli NM, Vadasz I. Novel concepts of acute lung injury and alveolar-capillary barrier dysfunction. *American journal of physiology Lung cellular and molecular physiology*. **2013**; 305: L665-81.
4. Aman J, Weijers EM, van Nieuw Amerongen GP, Malik AB, van Hinsbergh VW. Using cultured endothelial cells to study endothelial barrier dysfunction: Challenges and opportunities. *American journal of physiology Lung cellular and molecular physiology*. **2016**; 311: L453-66.
5. Komarova Y, Malik AB. Regulation of endothelial permeability via paracellular and transcellular transport pathways. *Annual review of physiology*. **2010**; 72: 463-93.
6. Fu P, Usatyuk PV, Lele A, Harijith A, Gregorio CC, Garcia JG, Salgia R, Natarajan V. c-Abl mediated tyrosine phosphorylation of paxillin regulates LPS-induced endothelial dysfunction and lung injury. *American journal of physiology Lung cellular and molecular physiology*. **2015**; 308: L1025-38.
7. Barabutis N, Dimitropoulou C, Birmpas C, Joshi A, Thangjam G, Catravas JD. p53 protects against LPS-induced lung endothelial barrier dysfunction. *American journal of physiology Lung cellular and molecular physiology*. **2015**; 308: L776-87.
8. Loirand G. Rho Kinases in Health and Disease: From Basic Science to Translational Research. *Pharmacological reviews*. **2015**; 67: 1074-95.
9. Kolluru GK, Majumder S, Chatterjee S. Rho-kinase as a therapeutic target in vascular diseases: striking nitric oxide signaling. *Nitric oxide : biology and chemistry / official journal of the Nitric Oxide Society*. **2014**; 43: 45-54.
10. Biro M, Munoz MA, Weninger W. Targeting Rho-GTPases in immune cell migration and inflammation. *British journal of pharmacology*. **2014**; 171: 5491-506.
11. Mohri M, Shimokawa H, Hirakawa Y, Masumoto A, Takeshita A. Rho-kinase inhibition with intracoronary fasudil prevents myocardial ischemia in patients with coronary microvascular spasm. *Journal of the American College of Cardiology*. **2003**; 41: 15-9.
12. Zhao J, Zhou D, Guo J, Ren Z, Zhou L, Wang S, Zhang Y, Xu B, Zhao K, Wang R, Mao Y, Xu B, Zhang X. Fasudil Aneurysmal Subarachnoid Hemorrhage Study G. Efficacy and safety of fasudil in patients with subarachnoid hemorrhage: final results of a randomized trial of fasudil versus nimodipine. *Neurologia medico-chirurgica*. **2011**; 51: 679-83.
13. Knipe RS, Tager AM, Liao JK. The Rho kinases: critical mediators of multiple profibrotic processes and rational targets for new therapies for pulmonary

- fibrosis. *Pharmacological reviews*. **2015**; 67: 103-17.
14. Duong-Quy S, Bei Y, Liu Z, Dinh-Xuan AT. Role of Rho-kinase and its inhibitors in pulmonary hypertension. *Pharmacology & therapeutics*. **2013**; 137: 352-64.
 15. Jiang X, Wang YF, Zhao QH, Jiang R, Wu Y, Peng FH, Xu XQ, Wang L, He J, Jing ZC. Acute hemodynamic response of infused fasudil in patients with pulmonary arterial hypertension: a randomized, controlled, crossover study. *International journal of cardiology*. **2014**; 177: 61-5.
 16. Mouchaers KT, Schalij I, de Boer MA, Postmus PE, van Hinsbergh VW, van Nieuw Amerongen GP, Vonk Noordegraaf A, van der Laarse WJ. Fasudil reduces monocrotaline-induced pulmonary arterial hypertension: comparison with bosentan and sildenafil. *The European respiratory journal*. **2010**; 36: 800-7.
 17. Ding RY, Zhao DM, Zhang ZD, Guo RX, Ma XC. Pretreatment of Rho kinase inhibitor inhibits systemic inflammation and prevents endotoxin-induced acute lung injury in mice. *The Journal of surgical research*. **2011**; 171: e209-14.
 18. Liu H, Chen X, Han Y, Li C, Chen P, Su S, Zhang Y, Pan Z. Rho kinase inhibition by fasudil suppresses lipopolysaccharide-induced apoptosis of rat pulmonary microvascular endothelial cells via JNK and p38 MAPK pathway. *Biomedicine & pharmacotherapy = Biomedecine & pharmacotherapie*. **2014**; 68: 267-75.
 19. Matute-Bello G, Winn RK, Jonas M, Chi EY, Martin TR, Liles WC. Fas (CD95) induces alveolar epithelial cell apoptosis in vivo: implications for acute pulmonary inflammation. *The American journal of pathology*. **2001**; 158: 153-61.
 20. Wang C, Armstrong SM, Sugiyama MG, Tabuchi A, Krauszman A, Kuebler WM, Mullen B, Advani S, Advani A, Lee WL. Influenza-Induced Priming and Leak of Human Lung Microvascular Endothelium upon Exposure to Staphylococcus aureus. *American journal of respiratory cell and molecular biology*. **2015**; 53: 459-70.
 21. Zahr A, Alcaide P, Yang J, Jones A, Gregory M, dela Paz NG, Patel-Hett S, Nevers T, Koirala A, Luscinskas FW, Saint-Geniez M, Ksander B, D'Amore PA, Argueso P. Endomucin prevents leukocyte-endothelial cell adhesion and has a critical role under resting and inflammatory conditions. *Nature communications*. **2016**; 7: 10363.
 22. Korthuis RJ, Anderson DC, Granger DN. Role of neutrophil-endothelial cell adhesion in inflammatory disorders. *Journal of critical care*. **1994**; 9: 47-71.
 23. Honda K, Kobayashi H, Hataishi R, Hirano S, Fukuyama N, Nakazawa H, Tomita T. Inhaled nitric oxide reduces tyrosine nitration after lipopolysaccharide instillation into lungs of rats. *American journal of respiratory and critical care medicine*. **1999**; 160: 678-88.
 24. Gong J, Wu ZY, Qi H, Chen L, Li HB, Li B, Yao CY, Wang YX, Wu J, Yuan SY, Yao SL, Shang Y. Maresin 1 mitigates LPS-induced acute lung injury in mice. *British journal of pharmacology*. **2014**; 171: 3539-50.

25. Gill SE, Rohan M, Mehta S. Role of pulmonary microvascular endothelial cell apoptosis in murine sepsis-induced lung injury in vivo. *Respiratory research*. **2015**; 16: 109.
26. Nozaki Y, Kinoshita K, Hino S, Yano T, Niki K, Hirooka Y, Kishimoto K, Funauchi M, Matsumura I. Signaling Rho-kinase mediates inflammation and apoptosis in T cells and renal tubules in cisplatin nephrotoxicity. *American journal of physiology Renal physiology*. **2015**; 308: F899-909.
27. Hannan JL, Matsui H, Sopko NA, Liu X, Weyne E, Albersen M, Watson JW, Hoke A, Burnett AL, Bivalacqua TJ. Caspase-3 dependent nitroergic neuronal apoptosis following cavernous nerve injury is mediated via RhoA and ROCK activation in major pelvic ganglion. *Scientific reports*. **2016**; 6: 29416.
28. He H, Yim M, Liu KH, Cody SC, Shulkes A, Baldwin GS. Involvement of G proteins of the Rho family in the regulation of Bcl-2-like protein expression and caspase 3 activation by Gastrins. *Cellular signalling*. **2008**; 20: 83-93.
29. Lai JM, Hsieh CL, Chang ZF. Caspase activation during phorbol ester-induced apoptosis requires ROCK-dependent myosin-mediated contraction. *Journal of cell science*. **2003**; 116: 3491-501.
30. Bhattacharya J, Matthay MA. Regulation and repair of the alveolar-capillary barrier in acute lung injury. *Annual review of physiology*. **2013**; 75: 593-615.
31. Stevens T, Garcia JG, Shasby DM, Bhattacharya J, Malik AB. Mechanisms regulating endothelial cell barrier function. *American journal of physiology Lung cellular and molecular physiology*. **2000**; 279: L419-22.
32. Huang Y, Tan Q, Chen R, Cao B, Li W. Sevoflurane prevents lipopolysaccharide-induced barrier dysfunction in human lung microvascular endothelial cells: Rho-mediated alterations of VE-cadherin. *Biochemical and biophysical research communications*. **2015**; 468: 119-24.
33. Stamatovic SM, Keep RF, Kunkel SL, Andjelkovic AV. Potential role of MCP-1 in endothelial cell tight junction 'opening': signaling via Rho and Rho kinase. *Journal of cell science*. **2003**; 116: 4615-28.
34. Mirza H, Wu Z, Teo JD, Tan KS. Statin pleiotropy prevents rho kinase-mediated intestinal epithelial barrier compromise induced by Blastocystis cysteine proteases. *Cellular microbiology*. **2012**; 14: 1474-84.
35. Gavard J, Gutkind JS. Protein kinase C-related kinase and ROCK are required for thrombin-induced endothelial cell permeability downstream from G α 12/13 and G α 11/q. *The Journal of biological chemistry*. **2008**; 283: 29888-96.
36. Tedgui A, Mallat Z. Anti-inflammatory mechanisms in the vascular wall. *Circulation research*. **2001**; 88: 877-87.
37. Millar FR, Summers C, Griffiths MJ, Toshner MR, Proudfoot AG. The pulmonary endothelium in acute respiratory distress syndrome: insights and therapeutic opportunities. *Thorax*. **2016**; 71: 462-73.
38. Charo IF, Ransohoff RM. The many roles of chemokines and chemokine receptors in inflammation. *The New England journal of medicine*. **2006**; 354: 610-21.

39. Bhatia M, Zemans RL, Jeyaseelan S. Role of chemokines in the pathogenesis of acute lung injury. *American journal of respiratory cell and molecular biology*. **2012**; 46: 566-72.
40. Guo F, Zhou Z, Dou Y, Tang J, Gao C, Huan J. GEF-H1/RhoA signalling pathway mediates lipopolysaccharide-induced intercellular adhesion molecule-1 expression in endothelial cells via activation of p38 and NF-kappaB. *Cytokine*. **2012**; 57: 417-28.
41. Anwar KN, Fazal F, Malik AB, Rahman A. RhoA/Rho-associated kinase pathway selectively regulates thrombin-induced intercellular adhesion molecule-1 expression in endothelial cells via activation of I kappa B kinase beta and phosphorylation of RelA/p65. *Journal of immunology (Baltimore, Md : 1950)*. **2004**; 173: 6965-72.
42. Liu SF, Ye X, Malik AB. Pyrrolidine dithiocarbamate prevents I-kappaB degradation and reduces microvascular injury induced by lipopolysaccharide in multiple organs. *Molecular pharmacology*. **1999**; 55: 658-67.
43. Shimada H, Rajagopalan LE. Rho kinase-2 activation in human endothelial cells drives lysophosphatidic acid-mediated expression of cell adhesion molecules via NF-kappaB p65. *The Journal of biological chemistry*. **2010**; 285: 12536-42.
44. Dauphinee SM, Karsan A. Lipopolysaccharide signaling in endothelial cells. *Laboratory investigation; a journal of technical methods and pathology*. **2006**; 86: 9-22.
45. Fukushima M, Nakamuta M, Kohjima M, Kotoh K, Enjoji M, Kobayashi N, Nawata H. Fasudil hydrochloride hydrate, a Rho-kinase (ROCK) inhibitor, suppresses collagen production and enhances collagenase activity in hepatic stellate cells. *Liver international : official journal of the International Association for the Study of the Liver*. **2005**; 25: 829-38.
46. Xu F, Xu Y, Zhu L, Rao P, Wen J, Sang Y, Shang F, Liu Y. Fasudil inhibits LPS-induced migration of retinal microglial cells via regulating p38-MAPK signaling pathway. *Molecular vision*. **2016**; 22: 836-46.
47. Long L, Ormiston ML, Yang X, Southwood M, Graf S, Machado RD, Mueller M, Kinzel B, Yung LM, Wilkinson JM, Moore SD, Drake KM, Aldred MA, Yu PB, Upton PD, Morrell NW. Selective enhancement of endothelial BMPR-II with BMP9 reverses pulmonary arterial hypertension. *Nature medicine*. **2015**; 21: 777-85.
48. Terkawi MA, Takano R, Kato K. Isolation and co-cultivation of human macrophages and neutrophils with Plasmodium falciparum-parasitized erythrocytes: An optimized system to study the phagocytic activity to malarial parasites. *Parasitology international*. **2016**; 65: 545-8.
49. Arita R, Hata Y, Nakao S, Kita T, Miura M, Kawahara S, Zandi S, Almulki L, Tayyari F, Shimokawa H, Hafezi-Moghadam A, Ishibashi T. Rho kinase inhibition by fasudil ameliorates diabetes-induced microvascular damage. *Diabetes*. **2009**; 58: 215-26.

Figure legends

Figure 1. Fasudil inhibited LPS-induced ROCK activation in lung. The results demonstrated fasudil reversed the phosphorylation of MYPT-1 and decreased the expression of ROCK1 in lungs of LPS-treated mice. (n = 3~4, * $p < 0.05$, ** $p < 0.01$ versus Con; # $p < 0.05$ versus LPS). Con: control; Fas: fasudil.

Figure 2. Fasudil ameliorated LPS-induced ALI and inflammation. (A) H&E staining showed severe inflammation in LPS group which was mitigated by fasudil pretreatment. The data indicated a high score for LPS-treated mice that fell down in fasudil-pretreated group. (B) GR-1 immunohistochemistry staining showed fasudil remarkably reduced neutrophil infiltration into lung interstitium and alveolar induced by LPS instillation. (C and D) Fasudil reversed LPS-induced increments of neutrophil numbers and MPO activities in BALF. (E and F) Fasudil prevented the production of TNF- α and IL-6 in serum. (G and H) Fasudil reversed the high levels of TNF- α and IL-6 in lungs tissues. (n = 6~8, * $p < 0.05$, ** $p < 0.01$ versus Con; # $p < 0.05$, ## $P < 0.01$ versus LPS). Scale bar: 30 μ m (H&E); Scale bar: 15 μ m (GR-1). Con: control; Fas: fasudil.

Figure 3. Fasudil reduced lung hyperpermeability induced by LPS. (A) Fasudil precondition significantly decreased LPS-induced protein leakage in BALF (n = 6~8). (B) Images and quantitative assessment of extravascular Evans blue dye of lungs demonstrated fasudil reversed exudation of extravascular Evans blue in lungs of

LPS-treated mice ($n = 4\sim 6$). (** $p < 0.01$ versus Con; ## $p < 0.01$ versus LPS). Scale bar: 0.5 cm. Con: control; Fas: fasudil.

Figure 4. Fasudil protected lung endothelial cells against LPS-induced dysfunction *in vivo*. **(A)** Immunofluorescence staining identified TUNEL⁺CD31⁺ cells as apoptotic endothelium (down row of panels, indicated by arrowheads). Fasudil pretreatment led to a significant reduction of apoptotic endothelial cells in lungs of LPS-challenged mice. **(B)** Western blot analysis suggested fasudil partially reversed LPS-induced down-regulation of VE-cadherin in lungs. ($n = 4$, ** $p < 0.01$ versus con; ## $p < 0.01$ versus LPS). Scale bar: 20 μm . VE-cad: VE-cadherin. Con: control; Fas: fasudil.

Figure 5. Fasudil reversed LPS-induced cultured human PMECs apoptosis. **(A)** Hoechst 33342 staining showed fasudil reversed human PMECs apoptosis induced by LPS ($n = 4$). **(B)** Fasudil pretreatment markedly inhibited caspase-3 activation in human PMECs exposed to LPS ($n = 3$). (** $p < 0.01$ versus Con; # $p < 0.05$, ## $p < 0.01$ versus LPS). Scale bar: 50 μm . C-caspase3: cleaved-caspase3. Con: control; Fas: fasudil.

Figure 6. Fasudil decreased LPS-induced human PMECs hyperpermeability. **(A)** Fasudil pretreatment reduced LPS-induced high permeability of FITC-dextran in human PMECs monolayer ($n = 4$). **(B and C)** Pretreated with fasudil reversed LPS-induced down-regulation of VE-cadherin ($n = 4$) and ZO-1 ($n = 3$). **(E and F)**

Immunofluorescence staining showed that fasudil prevented the loss of VE-cadherin and ZO-1 between adjacent human PMECs induced by LPS. (* $p < 0.05$, ** $P < 0.01$ versus Con; # $p < 0.05$, ## $p < 0.01$ versus LPS). Scale bar: 50 μm . VE-cad: VE-cadherin. Con: control; Fas: fasudil.

Figure 7. Fasudil suppressed human PMECs mediated neutrophil chemotaxis and neutrophil-endothelial adhesion. **(A)** Fasudil significantly inhibited neutrophil chemotaxis mediated by LPS-treated human PMECs ($n = 3$). **(B)** Fasudil suppressed the significant transcription of CXCL1, CXCL2 and CXCL8 ($n = 6$) in LPS-stimulated human PMECs. **(C)** Fasudil prevented the production of CXCL8 protein released from human PMECs exposed to LPS ($n = 6$). **(D)** Fasudil pretreatment suppressed neutrophil-endothelial adhesion induced by LPS treatment ($n = 5$). **(E)** Fasudil inhibited the overexpression of ICAM-1 in LPS-treated human PMECs ($n = 4$). (** $p < 0.01$ versus Con; # $p < 0.05$, ## $p < 0.01$ versus LPS). Scale bar; 20 μm . Con: control; Fas: fasudil.

Figure 8. Effects of fasudil on ROCK, NF- κB , and MAPK activation in LPS-challenged human PMECs. **(A)** Fasudil significantly suppressed LPS-induced MYPT-1 phosphorylation and ROCK1/2 up-regulation ($n = 4$). **(B)** Fasudil inhibited NF- κB p65 and $\text{I}\kappa\text{B}\alpha$ phosphorylation in LPS-challenged human PMECs ($n = 4$). **(C)** Fasudil significantly suppressed nuclear translocation of p65 in LPS-treated human PMECs. **(D)** Fasudil completely reversed LPS-elicited p38 phosphorylation, but

neither JNK nor ERK phosphorylation. (* $p < 0.05$, ** $p < 0.01$ *versus* Con; # $p < 0.05$, ## $p < 0.01$ *versus* LPS). Scale bar: 30 μm . Con: control; Fas: fasudil.



© 2017 by the authors. Licensee *Preprints*, Basel, Switzerland. This article is an open access article distributed under the terms and conditions of the Creative Commons by Attribution (CC-BY) license (<http://creativecommons.org/licenses/by/4.0/>).